Polymer-masking for controlled functionalization of carbon nanotubes†‡

Liangti Qu[a] and Liming Dai*[ab]

Received (in Cambridge, UK) 22nd May 2007, Accepted 29th June 2007
First published as an Advance Article on the web 13th July 2007
DOI: 10.1039/b707698c

An effective and versatile method for tube-length-specific functionalization of carbon nanotubes through a controllable embedment of vertically-aligned carbon nanotubes into polymer matrices is reported, which allows not only asymmetric functionalization of nanotube sidewalls, but also facile introduction of new properties (*e.g.* magnetic) onto the region-selectively functionalized carbon nanotubes.

Carbon nanotubes (CNTs) have been widely investigated for their application as reinforcement fillers in polymer composites.[1] The abilities to control their interaction with and orientation within polymer matrices are of paramount importance for tailoring the structure and property of the resultant nanocomposites.[2] In this context, the chemistry of CNTs has matured now for functionalizing *nonaligned* CNTs with various tailor-made surface characteristics to control their interaction with polymers and other materials.[3] In contrast, it is just a recent development to prepare polymer and *aligned* CNT composites with a controlled nanotube orientation in the polymer matrix.[4–10] A few recent studies have demonstrated that the embedment of *vertically-aligned* CNTs (VACNTs), either partially or fully, into appropriate matrices generated important synergetic effects that provide novel concepts and new properties for multifunctional applications, ranging from advanced chemical and biological sensors,[4,9] through smart membranes,[6] to flexible electronics.[5] While several different matrix materials, including poly(dimethylsiloxane) (PDMS),[5] polystyrene (PS),[6] poly(methyl methacrylate) (PMMA),[10] spin-on-glass,[7] and polydiene rubber,[8] have been used for embedding VACNTs, solution-coating has so far remained as the main method to achieve the embedment. Although the solution-based approach provides an effective means for fully embedding VACNTs through the whole nanotube length, it is still a big challenge to control the nanotube length being embedded (designed as: the embedment length) into an appropriate matrix (*e.g.* polymer). By simply heating a polymer thin film on the top of a VACNT array for infiltrating the melted polymer chains into the nanotube forest, we demonstrated in this study that the VACNTs can be embedded into the polymer matrix for any predetermined embedment length up to the whole nanotube length in a controllable fashion.

The controlled embedment of VACNTs into polymer matrices could not only lead to novel multifunctional nanocomposite materials and devices[4–10] but also open up new possibilities for region-selective functionalization of CNTs along the tube length, including *asymmetric sidewall-functionalization* (*vide infra*). Controlled functionalization of CNTs is essential for using CNTs as functional "building blocks" in various nanotube-based materials and devices.[11–15] We have previously reported *asymmetric end-functionalization* of CNTs by sequentially floating a substrate-free VACNT film on two different photoreactive solutions with only one side of the nanotube film being contacted with the photoreactive solution and exposed to UV light each time.[11] Here, we report the first simple, but effective and versatile, route to controlled functionalization of CNT sidewalls by embedding VACNTs into a polymer matrix at a predetermined embedment length, followed by modification of the polymer-free nanotube surface. As we shall see later, asymmetric sidewall-functionalization of carbon nanotubes can also be readily achieved through the same principle by sequentially polymer-masking VACNTs twice with only half of the nanotube sidewall being modified each time.

As schematically shown in Fig. 1(a), an appropriate polymer thin film (*e.g.* PS; M_w = 350 000; T_g (glass transition temperature)

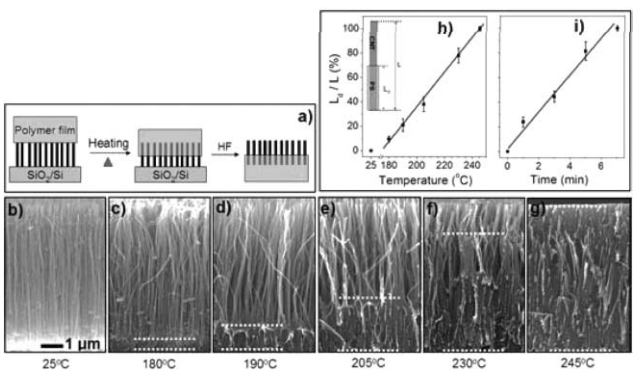

Fig. 1 (a) Schematic representation of the VACNTs embedded into a polymer matrix by thermal infiltrating the melted polymer into the nanotube forest; (b)–(g) SEM images of (b) the pristine VACNT array and (c)–(g) the VACNT array after being embedded into PS films by heating at different temperatures for 1 min. The dashed-line gaps crossing the polymer coated regions show the approximate embedment length for each of the PS-embedded VACNTs; (h) and (i) temperature and time dependence of the embedment length for VACNTs embedded into the PS matrix. (L: the nanotube length ($\sim$6 μm), L_d: the embedment length, which was estimated from the distance between the two dashed lines in each of the images shown in (c)–(g) and Fig. S1, ESI†.)

[a]*Department of Chemical and Materials Engineering, School of Engineering and UDRI, University of Dayton, 300 College Park, Dayton, OH, 45469-0240, USA. E-mail: ldai@udayton.edu; Fax: 937 229 3433; Tel: 937 229 2670*
[b]*Department of Chemistry, University of Dayton, 300 College Park, Dayton, OH, 45469, USA*

† Electronic supplementary information (ESI) available: Experimental details, characterization, and scheme of asymmetric functionalization of nanotube sidewalls. See DOI: 10.1039/b707698c

‡ The HTML version of this article has been enhanced with colour images.

$\approx$105 °C; T_m (melting point) $\approx$180 °C; T_c (decomposition temperature) $\approx$350 °C; thickness: $\sim$50 μm) was first placed on the top surface of a VACNT array (Fig. 1(a)) produced by pyrolysis of iron(II) phthalocyanine on a SiO_2/Si substrate.[16] Upon heating the SiO_2/Si substrate by an underlying hot plate to a temperature above T_m and below T_c, the melted PS film gradually filtrated into the nanotube forest (Fig. 1(a)) through a combined effect of the gravity and capillary forces. As expected, the infiltration depth (*i.e.* the embedment length) of PS into the nanotube forest depends strongly on the temperature and heating time. After a predetermined heating time, the polymer-infiltrated nanotube array was peeled off from the SiO_2/Si substrate in an aqueous solution of HF (10% wt)[16] to generate a free-standing film of VACNTs embedded into the PS matrix (Fig. 1(a), *cf.* Fig. S2, ESI‡). While Fig. 1(b) shows a typical scanning electron microscopic (SEM) image of the pristine VACNTs, Fig. 1(c)–(g) reproduce SEM images of the VACNTs embedded into PS films after being heated at different temperatures for 1 min. For the given infiltration time of 1 min, the embedment length increased with the heating temperature from *ca.* 10% coverage of the nanotube length at 180 °C up to the full length coverage at 245 °C (Fig. 1(c)–(g)). Fig. 1(h) shows a pseudo-linear relationship between the embedment length and the heating temperature covered in this study. For a given heating temperature (*e.g.* 195 °C), the embedment length was found to be directly proportional to the PS filtration time (*i.e.* heating time), as exemplified by Fig. 1(i) (*cf.* Fig. S1, ESI†). These results clearly show the feasibility for the tube-length-specific functionalization of CNTs by selectively functionalizing the polymer-free sidewall surface along the nanotube length *via* various physicochemical processes while the portion of the nanotube sidewall embedded into the polymer matrix is physically masked.

In view of the ease with which shape/size-controlled metal nanoparticles can be deposited onto carbon nanotube structures by our previously-reported surface-enhanced electroless deposition (SEED) method[13] and the effective action of the deposited nanoparticles as labeling centers for subsequent characterization, we demonstrated the tube-length-specific functionalization of CNTs by SEED deposition of Au nanoparticles onto each of the VACNTs partially embedded into the PS matrices shown in Fig. 1(c)–(f). In so doing, we first used the SEED method to deposit Au nanoparticles onto the constituent nanotubes in the PS-embedded VACNTs at the polymer-free region along their sidewalls. Thereafter, the polymer support was washed off with toluene to yield individual nanotubes region-selectively attached with the Au-nanoparticles, as shown in Fig. 2. The portions of the nanotube length covered by the Au nanoparticles seen in Fig. 2(a)–(d) consist well with the corresponding nanotube lengths extending out from the polymer matrices shown in Fig. 1(c)–(f), respectively. This indicates that the newly-developed polymer-masking technique can be effectively used to precisely control the portion(s) of the carbon nanotube length to be functionalized.

As mentioned earlier, the polymer-embedment/masking approach can also be used for *asymmetric* functionalization of the nanotube sidewall by sequentially masking VACNTs twice with only half of the nanotube length being modified each time. As schematically shown in Fig. 3(a)–(c) and Fig. S3, ESI,† we first used the SEED method[13] to deposit Pt *nanocubes* onto the polymer-free portion of the nanotube sidewalls of a PS-embedded VACNT array (Fig. 3(a) and Fig. S3(a,b), ESI†). Thereafter, a

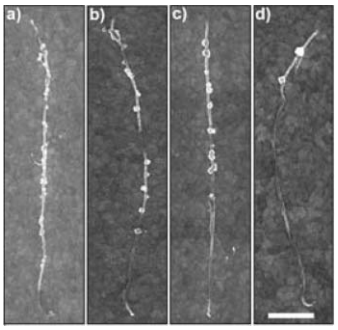

Fig. 2 SEM images of individual carbon nanotubes released out from the PS-embedded VACNTs by toluene washing after the Au nanoparticle deposition by SEED; (a)–(d) correspond to samples (c)–(f) in Fig. 1, respectively. Scale bar: 1 μm.

different polymer (*e.g.* poly(4-vinylpyridine) (PVP), M_w = 160 000, which is soluble in ethanol but insoluble in toluene) was used to fully cover the nanotube sidewalls attached with the Pt nanocubes (Fig. S3(c), ESI†), followed by turning over the polymer–VACNT composite film and quickly dissolving the PS coating in toluene (Fig. 3(b) and Fig. S3(c,d), ESI†). As a result, the other side of the nanotube outer wall originally embedded in the PS matrix was exposed for subsequent SEED deposition of *spherical* Pt nanoparticles (Fig. 3(c) and Fig. S3(e), ESI†). Subsequent removal of the PVP coating by ethanol washing led to *asymmetrically sidewall-functionalized* carbon nanotubes (Fig. 3(j) and Fig. S3(f), ESI†). While Fig. 3(d) and (g) clearly show the attachment of cubic nanoparticles onto the PS-embedded VACNTs, Fig. 3(e) and (h) reveal the intrinsic nanotube structure for the newly-exposed

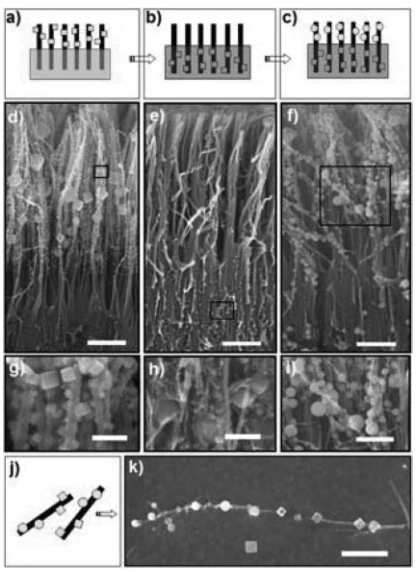

Fig. 3 (a)–(c) Schematic representations of VACNTs embedded into polymer matrices with Pt nanocubes and nanospheres region-selectively deposited along the nanotube length; (d)–(f) SEM images of the region-selectively-modified VACNTs corresponding to (a)–(c), respectively; (g)–(i) high-magnification SEM images of the selected squared areas in (d)–(f), respectively; (j) and (k), a schematic representation and SEM image of the resultant asymmetrically sidewall-functionalized carbon nanotubes, respectively, attached with Pt nanocubes and nanospheres along each half length of the same nanotube. Scale bars: (d–f) 1 μm; (g) 100 nm; (h) 200 nm; (i) 500 nm; and (k) 1 μm.

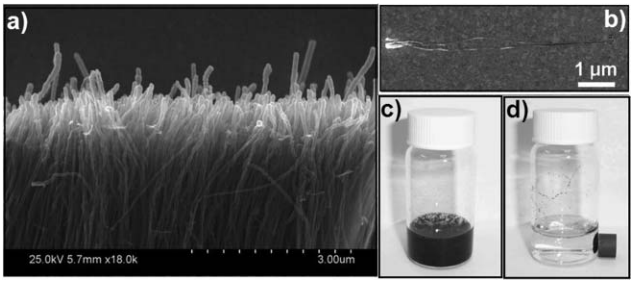

Fig. 4 SEM images of (a) the PS-embedded VACNT array with region-selectively sputter coated a thin layer of iron on the nanotube top end-tips and (b) individual constituent CNTs released out from the VACNT array of (a) by washing with toluene. Photos showing the dispersion behavior of the iron-sputter-coated CNTs in ethanol (c) without and (d) with an applied magnet. To remove the iron catalyst residues, the aligned CNT array shown in (a) has been turned over from the silicon wafer, followed by the water-plasma-etching and HCl treatment prior to the iron sputter coating, which caused the slight pull-out seen for some of the carbon nanotubes.

nanotube sidewalls on the top with the nanocube-attached region embedded into the bottom PVP layer. The spherical Pt nanoparticles subsequently deposited onto the PVP-embedded VACNTs were clearly evident in Fig. 3(f) and (i), from which a SEM image of the asymmetrically sidewall-functionalized carbon nanotube with Pt nanocubes attached on a half side of the nanotube length and nanospheres on the other half was obtained (Fig. 3(k)).

The embedment length of VACNTs into polymer matrices can be readily adjusted by controlling the experimental conditions (*e.g.* the heating temperature and time, *cf.* Fig. 1(h) and (i)) to allow for the controlled sidewall-functionalization of CNTs up to any predetermined length portions. Among many different materials that can be region-selectively deposited onto CNTs by the controlled sidewall-functionalization approach developed in this study, it is particularly interesting to region-selectively sputter coat a thin layer of iron onto the top tips of a PS-embedded VACNT array. By so doing, we found that the iron coating could impart magnetic properties to the nanotube tips. The newly-formed iron coating can be clearly seen at the tip region of both the PS-embedded VACNT array (Fig. 4(a)) and individual constituent nanotubes (Fig. 4(b)) released out from the VACNT array. After being dispersed in ethanol (Fig. 4(c)), these Fe-sputter-coated nanotubes showed strong attraction towards an external magnet, leading to an almost full separation of the CNTs out of the solution (Fig. 4(d)). Although the *as-synthesized* VACNTs showed certain magnetic properties arising from the residual iron catalyst particles,[17] most of the catalyst particles have been effectively removed by the HF etching for the substrate removal (*vide supra*) as well as the subsequent deliberate plasma-etching and HCl treatment[18] (ESI†). Together with the controlled functionalization of carbon nanotubes described above, therefore, these magnetization results indicate great potential for using the polymer-masking technique to develop various nanotube-based multifunctional materials and devices.

In summary, we have developed a simple, but effective and versatile, method for tube-length-specific functionalization of CNTs through a controllable embedment of VACNTs into polymer matrices. The controlled polymer-embedment/masking was achieved by melting an appropriate polymer film on the top of a VACNT array to allow the melted polymer chains to infiltrate into the nanotube forest under appropriate conditions (*e.g.* heating temperature and time). This polymer-masking approach has also been used not only for *asymmetrically* functionalizing nanotube sidewalls by sequentially masking VACNTs twice with only half of the nanotube sidewall being modified each time, but also for imparting magnetic properties to CNTs simply by region-selectively sputter-coating a thin layer of magnetic material (*e.g.* iron) onto the top-tips of VACNTs embedded into a polymer matrix (*e.g.* PS film). Therefore, the results reported in this communication represent a significant step forward towards controlled functionalization of CNTs for developing a wide range of novel nanotube-based multifunctional materials and devices.

This work was supported by NSF (NIRT-0609077; CMMI-0708055).

Notes and references

1 See, for example: (*a*) R. H. Baughman, A. A. Zakhidov and W. A. de Heer, *Science*, 2002, **297**, 787–792; (*b*) J. N. Coleman, U. Khan and Y. K. Gun'ko, *Adv. Mater.*, 2006, **18**, 689–706; (*c*) E. T. Thostenson, Z. F. Ren and T. W. Chou, *Composites Sci. Technol.*, 2001, **61**, 1899–1912.
2 (*a*) *Carbon Nanotechnology: Recent Developments in Chemistry, Physics, Materials Science and Device Applications*, ed. L. Dai, Elsevier, Amsterdam, 2006; (*b*) P. M. Ajayan, L. S. Schadler, C. Giannaris and A. Rubio, *Adv. Mater.*, 2000, **12**, 750–753; (*c*) H. D. Wagner, *Chem. Phys. Lett.*, 2002, **361**, 57–61; (*d*) C. Y. Li, L. Y. Li, W. Cai, S. L. Kodjie and K. K. Tenneti, *Adv. Mater.*, 2005, **17**, 1198–1202.
3 For recent reviews: (*a*) D. Tasis, N. Tagmatarchis, A. Bianco and M. Prato, *Chem. Rev.*, 2006, **106**, 1105–1136; (*b*) A. Hirsch, *Angew. Chem., Int. Ed.*, 2005, **41**, 1853–1859; (*c*) L. Dai, T. Lin, T. Ji and V. Bajpai, *Aust. J. Chem.*, 2003, **56**, 635–651; (*d*) J. L. Bahr and J. M. Tour, *J. Mater. Chem.*, 2002, **12**, 1952–1958; (*e*) Y.-P. Sun, K. Fu, Y. Lin and W. Huang, *Acc. Chem. Res.*, 2002, **35**, 1096–1104; (*f*) S. Niyogi, M. A. Hamon, H. Hu, B. Zhao, P. Bhowmik, R. Sen, M. E. Itkis and R. C. Haddon, *Acc. Chem. Res.*, 2002, **35**, 1105–1113.
4 C. Wei, L. Dai, A. Roy and T. B. Tolle, *J. Am. Chem. Soc.*, 2006, **128**, 1412–1413.
5 Y. J. Jung, S. Kar, S. Talapatra, C. Soldano, G. Viswanathan, X. S. Li, Z. L. Yao, F. S. Ou, A. Avadhanula, R. Vajtai, S. Curran, O. Nalamasu and P. M. Ajayan, *Nano Lett.*, 2006, **6**, 413–418.
6 B. J. Hinds, N. Chopra, T. Rantell, R. Andrews, V. Gavalas and L. G. Bachas, *Science*, 2004, **303**, 62–65.
7 C. V. Nguyen, L. Delzeit, A. M. Cassell, J. Li, J. Han and M. Meyyappan, *Nano Lett.*, 2002, **2**, 1079–1081.
8 L. C. Li, J. B. Yang, R. Vaia and L. Dai, *Synth. Met.*, 2005, **154**, 225–228.
9 J. Li, H. T. Ng, A. Cassell, W. Fan, H. Chen, Q. Ye, J. Koehne, J. Han and M. Meyyappan, *Nano Lett.*, 2003, **3**, 597–602.
10 N. R. Raravikar, L. S. Schadler, A. Vijayaraghavan, Y. P. Zhao, B. Q. Wei and P. M. Ajayan, *Chem. Mater.*, 2005, **17**, 974–983.
11 K. M. Lee, L. C. Li and L. Dai, *J. Am. Chem. Soc.*, 2005, **127**, 4122–4123.
12 Z. Wei, M. Kondratenko, L. H. Dao and D. F. Perepichka, *J. Am. Chem. Soc.*, 2006, **128**, 3134–3135.
13 (*a*) L. T. Qu, L. Dai and E. Osawa, *J. Am. Chem. Soc.*, 2006, **128**, 5523–5532; (*b*) L. T. Qu and L. Dai, *J. Am. Chem. Soc.*, 2005, **127**, 10806–10807.
14 S. J. Son and S. B. Lee, *J. Am. Chem. Soc.*, 2006, **128**, 15974–15975.
15 S. N. Li, P. G. He, J. H. Dong, Z. X. Guo and L. Dai, *J. Am. Chem. Soc.*, 2005, **127**, 14–15.
16 S. D. Huang, L. Dai and A. W. H. Mau, *J. Phys. Chem. B*, 1999, **103**, 4223–4227.
17 X. X. Zhang, S. Huang, L. Dai, R. Gao and Z. L. Wang, *J. Magn. Magn. Mater.*, 2001, **231**, L9–12.
18 S. M. Huang and L. Dai, *J. Phys. Chem. B*, 2002, **106**, 3543–3545.